Technical Note: Mobile accelerator guidance using an optical tracker during docking in IOERT procedures

Eugenio Marinetto[a)]
Department of Bioengineering and Aerospace Engineering, Universidad Carlos III, Madrid, Spain
Instituto de Investigación Sanitaria Gregorio Marañón, Madrid, Spain

Juan González Victores
Department of Systems Engineering and Automation, Universidad Carlos III, Madrid, Spain

Mónica García-Sevilla
Department of Bioengineering and Aerospace Engineering, Universidad Carlos III, Madrid, Spain
Instituto de Investigación Sanitaria Gregorio Marañón, Madrid, Spain

Mercedes Muñoz
Oncology Department, Hospital General Universitario Gregorio Marañón, Madrid, Spain
Facultad de Medicina, Universidad Complutense de Madrid, Madrid, Spain

Felipe Ángel Calvo
Instituto de Investigación Sanitaria Gregorio Marañón, Madrid, Spain
Oncology Department, Hospital General Universitario Gregorio Marañón, Madrid, Spain
Facultad de Medicina, Universidad Complutense de Madrid, Madrid, Spain

Carlos Balaguer
Department of Systems Engineering and Automation, Universidad Carlos III, Madrid, Spain

Manuel Desco and Javier Pascau
Department of Bioengineering and Aerospace Engineering, Universidad Carlos III, Madrid, Spain
Instituto de Investigación Sanitaria Gregorio Marañón, Madrid, Spain

(Received 22 February 2017; revised 14 July 2017; accepted for publication 14 July 2017; published xx xxxx xxxx)

Purpose: Intraoperative electron radiation therapy (IOERT) involves the delivery of a high radiation dose during tumor resection in a shorter time than other radiation techniques, thus improving local control of tumors. However, a linear accelerator device is needed to produce the beam safely. Mobile linear accelerators have been designed as dedicated units that can be moved into the operating room and deliver radiation *in situ*. Correct and safe dose delivery is a key concern when using mobile accelerators. The applicator is commonly fixed to the patient's bed to ensure that the dose is delivered to the prescribed location, and the mobile accelerator is moved to dock the applicator to the radiation beam output (gantry). In a typical clinical set-up, this task is time-consuming because of safety requirements and the limited degree of freedom of the gantry. The objective of this study was to present a navigation solution based on optical tracking for guidance of docking to improve safety and reduce procedure time.

Method: We used an optical tracker attached to the mobile linear accelerator to track the prescribed localization of the radiation collimator inside the operating room. Using this information, the integrated navigation system developed computes the movements that the mobile linear accelerator needs to perform to align the applicator and the radiation gantry and warns the physician if docking is unrealizable according to the available degrees of freedom of the mobile linear accelerator. Furthermore, we coded a software application that connects all the necessary functioning elements and provides a user interface for the system calibration and the docking guidance.

Result: The system could safeguard against the spatial limitations of the operating room, calculate the optimal arrangement of the accelerator and reduce the docking time in computer simulations and experimental setups.

Conclusions: The system could be used to guide docking with any commercial linear accelerator. We believe that the docking navigator we present is a major contribution to IOERT, where docking is critical when attempting to reduce surgical time, ensure patient safety and guarantee that the treatment administered follows the radiation oncologist's prescription. © *2017 American Association of Physicists in Medicine* [https://doi.org/10.1002/mp.12482]

Key words: docking, hard docking, image-guided surgery, IOERT, optical tracking, soft docking

1. INTRODUCTION

The main techniques for treatment of tumors are radiotherapy, chemotherapy, and surgery. In many clinical scenarios, tumor resection is the treatment of choice. However, recurrence makes the local control of the tumor a main concern to ensure patient survival. Intraoperative radiation therapy (IORT) enables precise application of high-dose radiation to the tumor bed during surgical resection,[1] thus improving local control of the tumor.[2–4] IORT can be delivered using electrons (intraoperative electron radiotherapy, IOERT), brachytherapy catheters (high-dose rate IORT, HDR-IORT),[2] or soft X-rays (50 kV).[5] IOERT, in particular, is able to deliver a higher dose in a shorter time than the other techniques. However, a linear accelerator device is needed to produce the beam safely.

The first clinical experiences with IOERT were carried out with nondedicated linear accelerators that were commonly used for external beam radiotherapy (EBRT). The patient had to be transported to the shielded linear accelerator room where specifically designed applicators were used to collimate the electron beam toward the tumor bed. However, patient transfer involved technical and safety concerns that were overcame with the appearance of commercial mobile linear accelerators in the late 1990s.

These devices were designed as dedicated units that could be moved into the OR, thus obviating the need to transfer the anesthetized patient during surgery. Mobile linear accelerators are compact and operate only in the electron mode (up to 10–12 MeV); therefore, they are safe in terms of protection from radiation, can be used in almost any existing OR and can be moved from one OR to another.[6] Consequently, the logistics and setting up of IOERT programs are easier and cheaper.[7,8] Examples of commercial devices include LIAC (Sordina IORT Technology, Aprilia, Italy), NOVAC-7/11 (Sordina IORT Technology, Aprilia, Italy), and Mobetron (IntraOp Medical Corp., Sunnyvale, CA, USA).[9,10]

Safe delivery of the correct dose is a key concern when using mobile accelerators. The procedure starts with the placement of the IOERT applicator (collimator) into the surgical area (i.e., inside the patient's anatomy). The angle, location, bevel, and diameter of the applicator are decided by the radiation oncologist prior to delivery. The applicator is generally fixed to the patient's bed, thus ensuring that radiation is delivered to the prescribed location, and the mobile accelerator is moved to dock the applicator to the radiation beam output (gantry). This task is critical for IOERT procedures[11] because the applicator could deviate from its current position during docking, thus altering the distribution of the dose delivered. As Beddar and colleagues suggest in,[7] "the geometric accuracy of treatment delivery using a mobile unit will depend solely on the accuracy of the docking." In a typical clinical scenario, this task is time-consuming owing to safety requirements and the limited degrees of freedom (DoF) of the gantry. To facilitate docking, some commercial devices provide various DoFs to adapt the beam trajectory to the prescribed applicator location and, optionally, dedicated guiding systems. Docking techniques can be divided into two main groups: hard and soft docking.

In hard docking (used, e.g., by the NOVAC-7 and LIAC systems), the electron applicator is divided into two parts: at the time of IOERT the upper part is directly connected and fixed to the gantry of the mobile linear accelerator while the lower part is placed in contact with the tumor bed to be irradiated. Then, the therapist moves the machine toward the patient (selecting the correct position of the different DoF) simultaneously aligning and minimizing the distance between the two components of the applicator. This task is performed continuously by the therapist for safety reasons to prevent potential injury to the patient.[6] Once this procedure is complete, the two parts are then firmly connected to guarantee the precise alignment of the radiation beam axis. The time needed for the whole-docking procedure depends on the application and can take up to ~15 min.[12]

In soft docking, the machine is decoupled from the applicator to ensure the patient's safety in the event of uncontrolled movement of the machine. The difficulty then arises as to how to align the central axis of the linear accelerator with that of the applicator and set the correct treatment distance. This requires an optical or mechanical alignment system. Many soft-docking systems have been described in the literature.[8,11,13,14] The technique used in Mobetron was evaluated in Börjk et al[11] and Beddar et al.[12] In terms of treatment accuracy, angular displacements were found to be critical for ensuring dose distribution flatness and symmetry. Furthermore, docking time was slightly reduced to 10 min (mean).

The limited DoFs of the gantry design could increase docking time. Commercial mobile accelerators are not isocentric *per se,*[7] thus making docking a cumbersome task for the operators in the OR. In fact, in some cases, and because of the limitations of the OR for movement of the mobile accelerator, some applicator positions/orientations are unreachable. In these cases, the patient's bed is usually moved closer to the mobile unit.

Consequently, new techniques are required to improve the safety and speed of the docking procedure, reduce surgical time, and avoid unreachable positions. The oncology department at Hospital Gregorio Marañón (Madrid, Spain) performs IOERT regularly in a nondedicated OR using Sordina's LIAC [Fig. 1(d)]. The mobile unit has five DoFs: gantry rotation angle, tilt angle, height, translational shift, and wheel rotation (hard docking). The two-rotation axes of the gantry intersect at a point outside the collimator axis, thus making the docking procedure poorly intuitive in many cases. This limitation increases docking time by up to 15 min depending on the location of the tumor, even for trained technicians.[15]

The objective of this work was to present a navigation solution based on optical tracking for the guidance of docking that is expected to improve safety and reduce procedure time. The solution presented tracks the applicator localization inside the OR, computes the movements that the mobile linear accelerator should perform to align the applicator and the radiation gantry and warns the oncologist if the setup is unreachable by the available DoFs. The navigation system

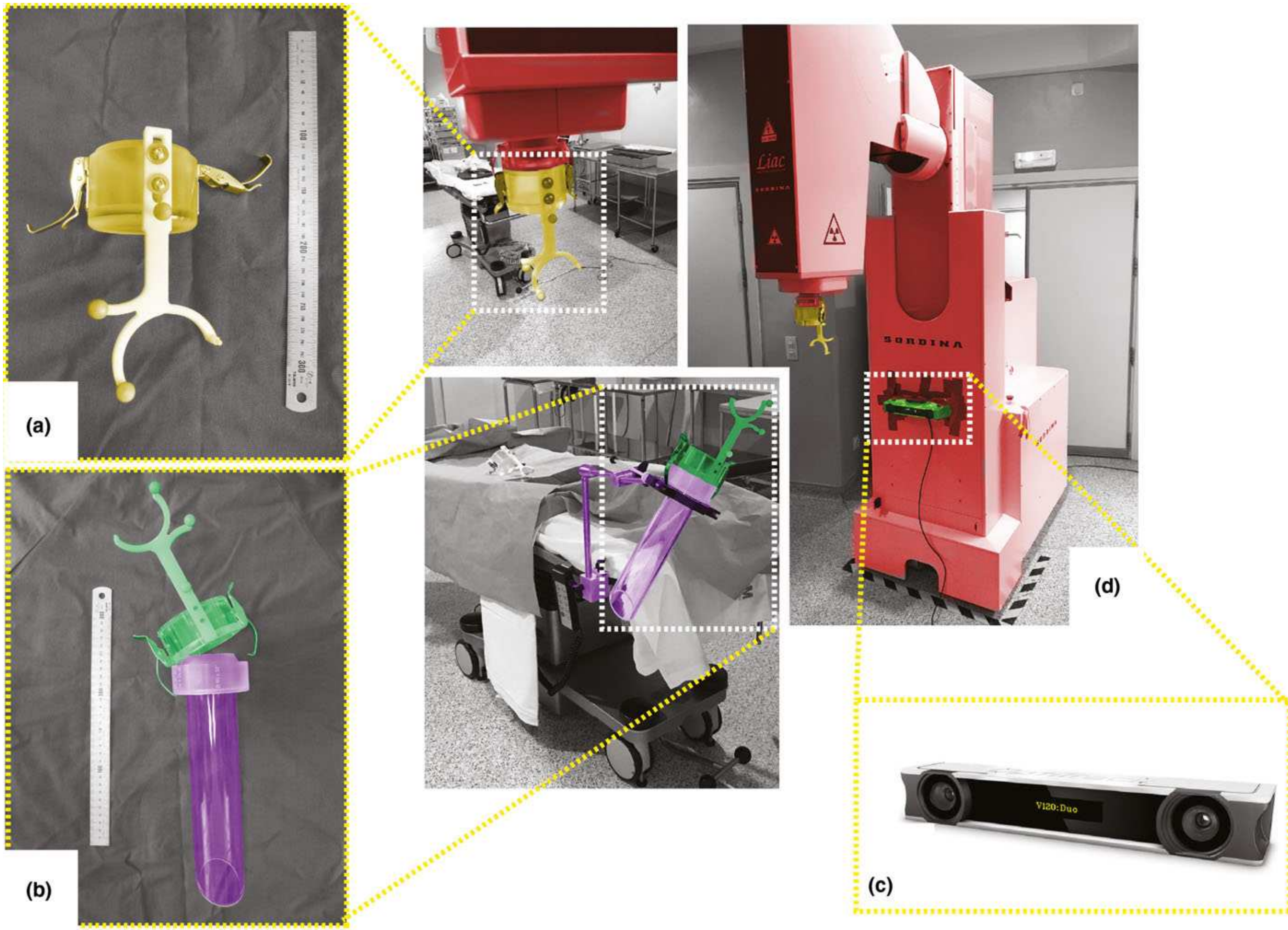

FIG. 1. Complete navigation set-up: (a) Calibration tool and associated tracking rigid body, (b) IOERT applicator (lower part) and associated tracking rigid body (upper part), (c) OptiTrack V120:Duo[16], and (d) IOERT applicator and Sordina LIAC with the attached OptiTrack V120:Duo (c) and calibration tool (yellow).

was implemented using an in-house software application to guide the technician during the docking procedure. The approach feasibility was assessed on simulated cases and tested on three cases emulating real clinical scenarios, where docking time was recorded for evaluation purposes.

2. MATERIALS AND METHODS

2.A. Navigation setup and linear accelerator kinematics

We used the OptiTrack V120:Duo optical tracker (NaturalPoint, OR, USA) [Fig. 1(c)] to track the radiation applicator [Fig. 1(b)]. This system has two cameras embedded in fixed body that provides the position of the passive retro-reflective markers, which are small spheres coated with IR-reflective material from NaturalPoint (7/16'' hard model[16]). The position of the tracked tools is obtained in real time using the tracker manufacturer's software.

The IOERT accelerator used in our institution is a LIAC 12 device (Sordina, Aprilia, Italy). We placed the tracker in the front part of the accelerator [Fig. 1(d), red] to track the calibration tool [Fig. 1(a)] and the IOERT applicator [Fig. 1(b)]. The main idea for navigation is to track the treatment applicator localization using the attached rigid body [Fig. 1(b), green] and estimate the movements of the linear accelerator toward the applicator localization for a correct docking.

LIAC 12 has five DoFs (Fig. 2): base shift (Fig. 2, DoF-1), base rotation (Fig. 2, DoF-2), gantry rotation (Fig. 2, DoF-3), gantry height (Fig. 2, DoF-4), and gantry tilt (Fig. 2, DoF-5). When an IOERT procedure is performed, only the mobile unit [Fig. 2(b)] is moved into the OR during surgery, and the hard-docking technique is used. Note that the tracker is attached to the base of the mobile unit [Fig. 1(c)]. Therefore, when the base is driven, the optical tracker is moved jointly since both elements are attached together. LIAC can move the complete mobile unit by shifting and rotating the base [Fig. 2(b), DoF-1 and DoF-2] with no restrictions. However, the gantry's movements are limited [Fig. 2(c), DoF-(3 to 5)].

The Denavit-Hartenberg (DH) convention[17] is widely used in the literature to describe the kinematics of robotic arms.

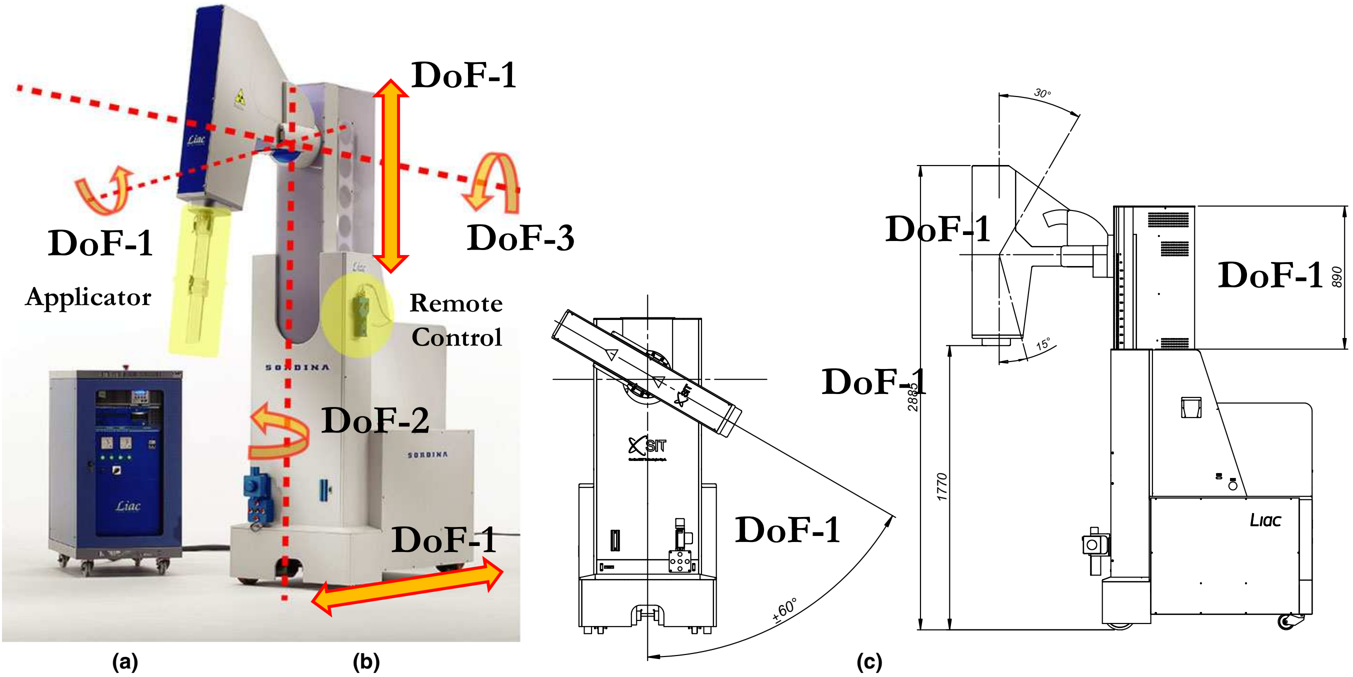

FIG. 2. LIAC 12 (Sordina, Aprilia, Italy). (a) Control unit. (b) Mobile unit. Degrees of freedom: (DoF-1) base shift, (DoF-2) base rotation, (DoF-3) gantry rotation, (DoF-4) gantry height and (DoF-5) gantry tilt. (c) Gantry movement limits. Shaded: Radiation applicator and remote control. (Images courtesy of Sordina).

DH associates each DoF with a single joint, which is defined by a transformation that depends on a unique parameter (q). Robotic arms are defined as a chain of joints. Depending on the joint type (rotation or shift), the parameter (q) that defines the position of the joint is measured in degrees (rotation) or meters (shift) with respect to its outset position. To define the kinematics of a complete chain of joints (i.e., robotic arm), the DH nomenclature starts from the basis that it is fixed in space (where the robotic arm is attached) and defines the associated transformation to the first joint. This transformation depends on the control parameter (q, rotation or shift) that characterizes its movement and relates the base and joint coordinate systems by the transformation ${}^{Joint_1}T_{Base}(q_1)$. The next joint is then defined by a new transformation that depends on another unique parameter (q_2). This transformation relates the current and the previous joint coordinate systems (${}^{Joint_2}T_{Joint_1}(q_2)$). The process is repeated for each joint of the robotic arm. Using this notation, the end-joint coordinate system (i.e., robotic arm tip) is related to the base's coordinate system by the product in (Eq. 1):

$$ {}^{Joint_N}T_{Base}(\boldsymbol{q}) = \prod_{i=0}^{N} {}^{N-i}T_{N-1-i}[q_{N-i}] \tag{1} $$

where ${}^{Joint_N}T_{Base}(\boldsymbol{q})$ is the transformation that relates the coordinate system of the base and the robotic arm tip and depends on the vector of parameters $\boldsymbol{q} = [q_1, \ldots, q_N]$., is the number of total joints, q_i the joint parameter (rotation angle/shift) of the i-th joint and ${}^{i}T_{i-1}[q_i]$ relates the joint (i) and ($i-1$) coordinate systems when the joint is at the position defined by i. Note that for $q_i = 0.0, i \in [1, N]$ (i.e., outset position) the transformation ${}^{Joint_N}T_{Base}$ relates the base coordinate system to the robotic arm tip.

In kinematic terms, LIAC can be considered a robotic arm with 5 degrees of freedom. Following the DH convention, we can describe the accelerator chain using five joints, one for each DoF. However, the kinematic chain of the gantry is attached to the base of the mobile unit [Fig. 2(b)], which is also mobile. To represent this mobility in DH nomenclature, we added four auxiliary joints as in Fig. 3 (i.e., Joints 1 to 4). From this DH characterization standpoint, the accelerator can perform seven movements to reach the target applicator and complete the docking process. Using the DH characterization described above, the location of the gantry with respect to the outset position is completely defined by the parameters $\boldsymbol{q}$ when the LIAC is moved for docking.

The LIAC installed in our OR can only be moved over a 2-m^2 surface to prevent collisions, owing to the restriction imposed by the OR ceiling height. This restriction is represented by the limitation of the movements of the base rotation to ±45° (Joints 1 and 3) and the base shift to ±0.3 m (Joints 2 and 4). Note that the maximum distance that the LIAC can be moved from its outset position is 0.6 m following a straight path that, combined with the base rotation restriction (±45°), defines a semicircle of radius 0.6 m, which respect the 2-m^2 restriction. These parameters could be adapted for any OR with different restrictions.

Once Joints 1–4 are fixed, the gantry's DoF (Joints 5–7) restrict the possible docking orientations. Therefore, in a typical operation, some docking arrangements are not possible

(a)

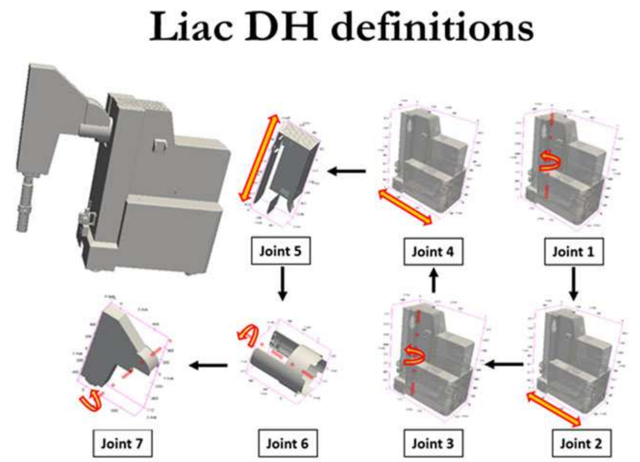

(b)

	Joint 1	Joint 2	Joint 3	Joint 4	Joint 5	Joint 6	Joint 7
Rotation Z	0º + q_1	90º	0º + q_3	0º	0º	0º + q_6	-90º + q_7
Traslation Z	0	0 + q_2	0	0 + q_4	0 + q_5	d_1 (1.325 m)	d_2 (0.3 m)
Traslation X	0	0	0	0	0	0	0
Rotation X	0º	90º	-90º	90º	-90º	90º	-90º
Minimum	-45º	-0.3 m	-45º	-0.3 m	0	-60º	-30º
Maximum	45º	0.3 m	45º	0.3 m	0.89 m	60º	15º
	Extra joint for convenience		Current Liac Joints				

FIG. 3. Denavit-Hartenberg parameters for the Sordina LIAC 12 device. (a) Defined Joints and movements for the kinematic chain. (b) Table of D-H parameters (q_i) and limits of each joint.

unless the mobile unit or the patient is appropriately reoriented. This is one of the main factors increasing docking time in clinical cases.

2.B. Navigation system calibration

Figure 4 shows all the geometric transformations involved in the navigation solution. The transformation ${}^{LIAC}T_G$ relates the position of the gantry geometrically with respect to the accelerator. According to DH parameters, ${}^{LIAC}T_G$ (Fig. 4) depends on the parameters $\boldsymbol{q}$ (Eq. 2).

$$ {}^{LIAC}T_G = {}^{LIAC}T_G(\boldsymbol{q}) \tag{2} $$

To obtain the transformation ${}^{Tr}T_{LIAC}$ (Fig. 4), which relates the tracker (Tr) and LIAC accelerator coordinate systems, a calibration step should be performed prior to navigation. We used a custom-designed calibration tool attached to the LIAC gantry [Fig. 1(a)] for this purpose which is localized by the tracker (${}^{G}T_{Tr}$).

Before calibration, the LIAC is moved to the outset position ($q_i = 0.0, i \in [1, 7]$). The calibration process consists of three acquisitions. First, (1) we gather the localization of the gantry (${}^{G}T_{Tr}$) at the LIAC outset position. Then, (2) we rotate the gantry (joint 7) from –60° to 60° and record its trajectory. Finally, (3) we return to the outset position and record the gantry location while only Joint 5 (gantry height) is moved from 0 to 0.89 m. For the outset gantry location, we record 1000 samples, whereas for the calibration trajectories of Joints 7 and 5, we record tracking data at the tracker's

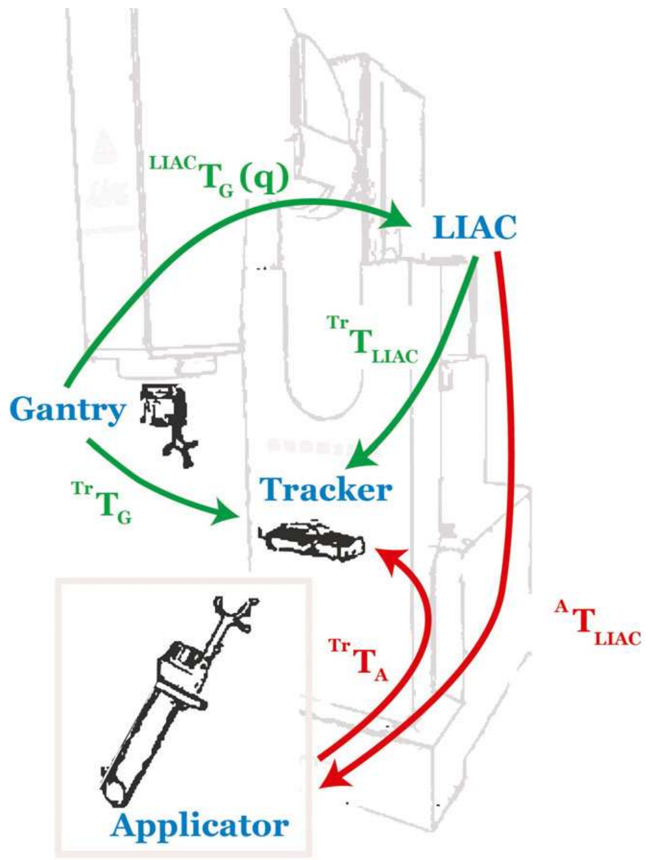

FIG. 4. Pertinent coordinate transformations of the docking navigation setup.

maximum frame rate by moving the joints at maximum (and constant) speed.

We then estimate the center of the gantry coordinate system in the tracker coordinate system as the mean of the acquired location samples at the outset position (1). This central location populates the last column of the transformation ${}^{Tr}T_{LIAC}$ (Fig. 4). Orientation is extracted using two trajectory acquisitions, namely, rotation and height shift of the gantry (2 & 3). Note that both acquisitions are in perpendicular planes. The normal vectors to the planes define two axes of the gantry coordinate system — $\boldsymbol{x}$ and $\boldsymbol{y}$. The third axis of rotation (z) is computed based on the cross product following right-handed geometry notation ($\mathbf{x} \times \mathbf{y} = \mathbf{z}$). Vectors $\boldsymbol{x}$, $\boldsymbol{y}$ and z populate the orientation matrix of ${}^{Tr}T_{LIAC}$. When the calibration process is finished, the transformation ${}^{Tr}T_{LIAC}$ is fully estimated and can be used to compute the location of the applicator in the accelerator coordinate system as shown in (Eq. 3).

$$ {}^{A}T_{LIAC} = {}^{A}T_{Tr} \cdot {}^{Tr}T_{LIAC} \quad (3) $$

2.C. Docking navigation

After a calibration, the proposed navigation set-up is ready to assist in the docking procedure. First, the applicator [Fig. 1(b)] is fixed to the tumor bed, and the patient's bed is moved closer to the accelerator. The objective of docking is to move the LIAC ($\boldsymbol{q}$) to fulfill the condition of (Eq. 5), where the applicator and gantry coordinate systems are coinciding.

$$ {}^{A}T_{LIAC} \equiv {}^{G}T_{LIAC}(\boldsymbol{q}) \quad (4) $$

In mathematical terms, docking can be written as a minimization problem (Eq. 5) using the navigation set-up proposed, as follows:

$$ \boldsymbol{q} = [q_1, q_2, q_3, q_4, q_5, q_6, q_7] \\ \min_{\boldsymbol{q}} \| {}^{A}T_{LIAC} - {}^{G}T_{LIAC}(\boldsymbol{q}) \|_M \textit{such as } q_i \in [min_i, max_i], i \in [1,7] \quad (5) $$

where $\boldsymbol{q}$ are the accelerator moving parameters, $[min_i, max_i]$ the limits of parameter q_i (Table I) and M a metric that measures the transformation differences.

Solving the inverse kinematics problem of Eq. 5 produces the optimal docking accelerator parameters ($\boldsymbol{q}$) to align the LIAC's gantry and the radiation applicator under safe conditions, including speed constraints and restricted to the collision-free area of the OR. We used the L2 norm as the metric (M) and the Sequential Least SQuares Programming optimization algorithm (SLSQP) to estimate the docking parameters.[18]

Given the limits of the accelerator DoF, the solution to Eq. 5 could not produce an ideal match (i.e., Eq. 4). To quantify the docking error of the solution, we estimated *position* and *rotation error* of the given solution. The *position error* measures the Euclidean distance of the solution and the current applicator position at the center of the applicator bevel.

Table I. Docking time at Hospital General Universitario Gregorio MaraÑÓn (Madrid, Spain) for different cases and locations.

Localization	Docking time
Rectum	05:50 min
Rectum	05:20 min
Rectum	05:40 min
Right breast	09:40 min
Left breast	06:30 min
Rectum	06:00 min
Right breast	18:00 min[a]
Testicles	08:00 min
Right breast	13:00 min[a]
Mean	8:26 min

[a]Cases considered extremely time-consuming.

The *rotation error* measures the difference in the angle on the applicator longitudinal axis. Before the docking procedure, these parameters are given to the radiation oncologist for assessment. Hence, providing the oncologist with valuable information prior to the docking procedure that could save time if estimated errors are not considered adequate for the procedure. If the errors are too large, the physician could decide in advance to re-orient the patient's bed differently and estimate new docking parameters with a lower error (better accuracy).

2.D. Navigation software

We integrated the navigation system into a software application that connects all the necessary elements and provides a user interface. This integration was implemented using the TREK surgical navigation platform[19,20] using the BiiGOptitrack library[21] to interface with the tracker and collect the tracking information.

The application developed has two main tabs, namely, *calibration* [Fig. 5(a)] — to follow the steps described in Section 2.B and *guidance* [Fig. 5(b)] — to guide the docking procedure. Once the oncologist has defined the site of treatment for the applicator, the optimal docking parameters ($\boldsymbol{q}$) are estimated and shown in the user interface [Fig. 5(b), *Objective column*].

2.E. Evaluation of docking navigation

We measured the docking time for standard clinical IOERT treatments over 1 month in our dedicated OR. Specifically, we measured the time interval between when the applicator is fixed to the patient's bed until final docking.

Furthermore, we assessed the accuracy of the docking in terms of position and rotational error in a computer simulation-based evaluation. In each simulated docking problem (N = 4000), the applicator was randomly positioned 2 m away from the LIAC into a 0.5 × 0.4 m rectangle and rotated ±50° from the vertical axis in random direction. We used the developed system to solve the path,

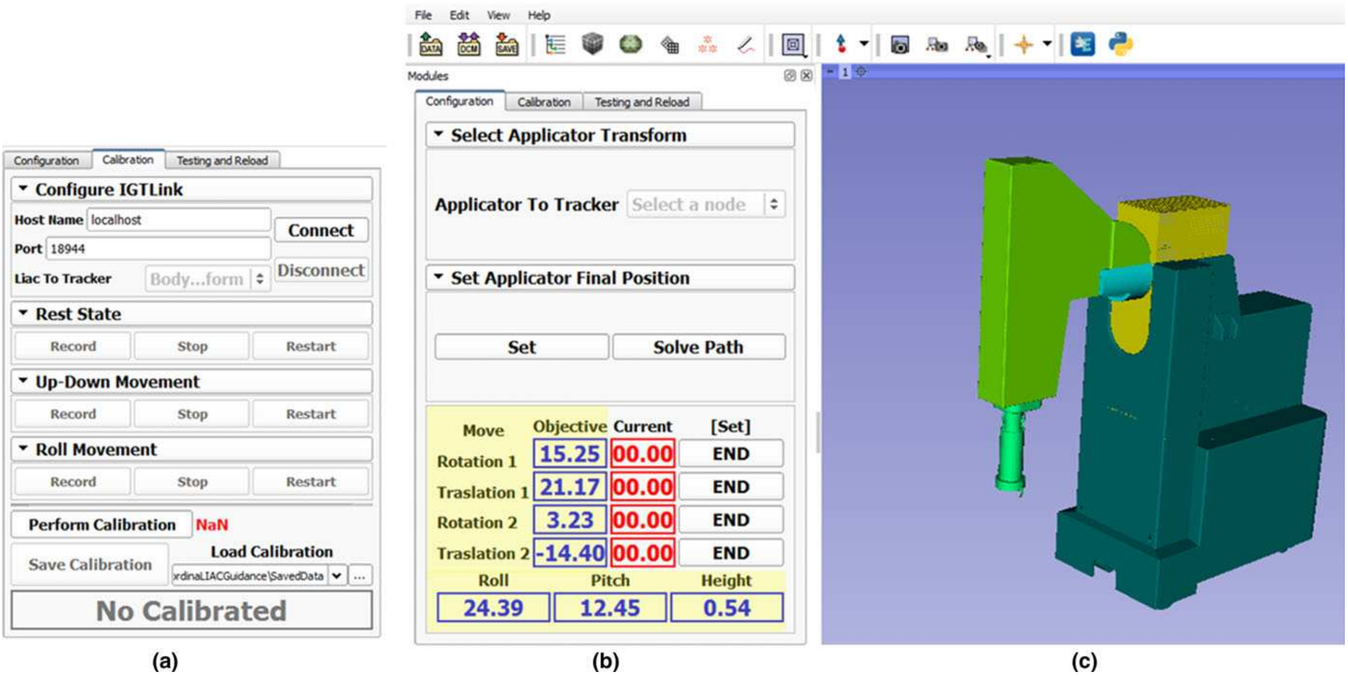

FIG. 5. IOERT LIAC docking navigation application. (a) Calibration interface, (b) Docking navigation panel showing the docking parameters (shaded) and (c) 3D model of LIAC and target applicator position showing the docking set-up.

measured position and rotational error and estimated the docking time using the maximum motor speed for each DoF of the machine. To take into account unreachable docking arrangements, we considered only cases with position and rotational errors below 1 mm and 0.1°, respectively.

In addition, we ran an experimental setup using the navigation software in the OR in which we emulated three clinical cases (left breast, right breast and rectal cancer). The applicator was positioned based on the experience of a qualified radiotherapist. We calibrated the system following the workflow described above and estimated the docking parameters using the software application. A skilled IOERT technician controlled the accelerator movements following the developed navigation system instructions with no other guidance, and a clinician evaluated the suitability of docking. On each experimental setup, we measured the docking time for assessment purposes.

3. RESULTS

Table I shows the docking times recorded in the OR for IOERT procedures over 1 month at Hospital General Universitario Gregorio Marañón (Madrid, Spain). As we can see, the mean time of 8:26 min shows that docking is a time-consuming task. According to the physicians, longest cases, which are right breast interventions, are particularly complicated owing to the spatial limitations of the OR (Table I, red). Such cases often lead to unreachable docking arrangements by the accelerator, with the result that the patient must be moved closer or even reoriented, thus increasing docking time considerably (see Table I).

Table II shows the docking time for the three simulated cases. Using our navigation system, the maximum docking time was below 5 min, which is shorter than all the clinical cases recorded in Table I. In one case (right breast, Table II), the estimated docking rotational error was too large (>15° applicator axis) owing to an unreachable orientation. This case was recalculated using our software after moving the patient (and the fixed applicator) closer to the accelerator. For all the experimental cases, the docking parameters were estimated correctly, and the technician performed the docking using the navigation pane with no major issues.

Regarding the simulation-based assessment, the results showed a 25.55% of unreachable docking arrangements which demonstrates the high probability of facing this problem in a real scenario. This could lead to the repetition of the docking process, hence extending surgical time. The navigation system provides the estimated error prior to the actual docking task, enabling the clinicians to arrange the patient to a new position before repeating the calculation of the docking parameters. For the reachable simulated cases, we found a position error of 0.0023 ± 0.0373 mm (mean ± std.), a rotational error of $6.77\ 10^{-5} \pm 230.53\ 10^{-5}$ degrees

TABLE II. Docking time for simulated clinical cases using the navigation system.

Localization	Docking time
Rectum	03:20 min
Right breast	04:10 min
Left breast	03:30 min
Mean	3:40 min

(mean ± std.), and an estimated docking time of 2.3 ± 0.4 min (mean ± std.).

4. DISCUSSION AND CONCLUSIONS

We present a navigation solution based on optical tracking as a guide for docking that improves safety and reduces procedure time. To our knowledge, this is the first docking navigation system for mobile linear accelerators. Our solution, which can track the applicator location inside the OR, computes the movements needed for the LIAC mobile unit to correctly align the applicator and the radiation gantry. In case the set-up is unreachable because of DoF limitations, the system can notify the user to save procedure time, thus improving performance of IOERT. Note that it can also be applied to other linear accelerators or even for soft-docking guidance. However, it requires specific tracking tools and a previous system calibration.

The presented docking navigator could be built together with the mobile accelerator unit to reduce calibration time and be adapted to any specific movement limitations in the OR. This paper presents a proof of concept to demonstrate the feasibility of using an optical tracker to guide the docking task. A key limitation of this system is the user's reliance on the control of the accelerator's DoF. The movements of the mobile unit are not controlled by stepper motors. Hence, they cannot reliably locate the mobile unit arrangement. Nevertheless, our system allows estimating the docking parameters at any time, even after performing some of the movements, which may overcome this limitation. Our simulation results showed an estimated docking time of 2.3 min. However, during real experimental setups, docking time was increased ~1 min (Table II) that could be partially due to the named limitation. Introducing stepper motors or encoders for feedback on linear and angular position could solve this problem, since placement of the mobile unit would be used by the navigation system to guide the user toward optimal estimates of rotations and shifts. Also, note that our system facilitates the docking task, however, the surgical team is expected to avoid collisions with the patient for safety reasons.

The presented docking guidance system complements the previously presented IOERT navigation solution.[22–24] In fact, both solutions could be connected to the IOERT treatment planning system, thus improving automation of IOERT procedures. Such an approach could overcome human data transmission errors and make it possible to monitor potential mistakes in human actions (risk factors previously identified in[25]), thus improving quality control in these interventions.

The system we present safeguards against OR limitations (ceiling), calculates the optimal DoF arrangement of the accelerator and reduces docking time. These benefits, which are shown in our results, have encouraged us to confirm them through further study in clinical cases in the near future. We think that the docking navigator we present is an important contribution to the IOERT community, where docking is critical for reducing surgical time, ensuring patient safety and guaranteeing that the treatment administered follows the prescription of the radiotherapist.

ACKNOWLEDGMENTS

The research was supported by projects TEC2013-48251-C2-1-R, DTS14/00192, PI15/02121 (Ministerio de Economía y Competitividad, Instituto de Salud Carlos III and European Regional Development Fund "Una manera de hacer Europa") and TOPUS-CM S2013/MIT-3024 (Comunidad de Madrid). The authors also extend their gratitude to the radiotherapy technicians at Hospital General Universitario Gregorio Marañón and to Laura Sanz for their support.

[a]Author to whom correspondence should be addressed. Electronic mail: emarinetto@hggm.es.

REFERENCES

1. Calvo FA. Intraoperative irradiation: precision medicine for quality cancer control promotion. *Radiat Oncol*. 2017;12:36.
2. van de Voorde L, Delrue L, van Eijkeren M, de Meerleer G. Radiotherapy and surgery-An indispensable duo in the treatment of retroperitoneal sarcoma. *Cancer*. 2011;117:4355–4364.
3. Haddock MG, Miller RC, Nelson H, et al. Combined modality therapy including intraoperative electron irradiation for locally recurrent colorectal cancer. *Int J Radiat Oncol Biol Phys*. 2011;79:143–150.
4. Calvo FA, Meirino RM, Orecchia R. Intraoperative radiation therapy. Part 2. Clinical results. *Crit Rev Oncol Hematol*. 2006;59:116–127.
5. Vaidya JS, Baum M, Tobias JS, Morgan S, D'Souza D. The novel technique of delivering targeted intraoperative radiotherapy (Targit) for early breast cancer. *Eur J Surg Oncol*. 2002;28:447.
6. Gunderson LL, Willett CG, Calvo FA, Harrison LB. *Intraoperative Irradiation: Techniques and Results*. Springer; 2011. https://books.google.com/books?id=NKbr_my9EkgC&pgis=1. Accessed November 13, 2016.
7. Beddar AS, Biggs PJ, Chang S, et al. Intraoperative radiation therapy using mobile electron linear accelerators: report of AAPM Radiation Therapy Committee Task Group No. 72. *Med Phys*. 2006;33:1476.
8. Chandriah H. Mobetron, Health Technology Assessment Section (MaHTAS). 2010. https://www.google.es/url?sa=t&rct=j&q=&esrc=s&source=web&cd=1&cad=rja&uact=8&ved=0ahUKEwij3Yru0rPVAhWJuhQKHaIEBJYQFggoMAA&url=http%3A%2F%2Fwww.moh.gov.my%2Findex.php%2Fdatabase_stores%2Fattach_download%2F347%2F132&usg=AFQjCNFVtkJdIDz1tuSbt08GQWOqjHUKMQ. Accessed February 22, 2017.
9. Calvo FA, Meirino RM, Orecchia R. Intraoperative radiation therapy first part: rationale and techniques. *Crit Rev Oncol Hematol*. 2006;59:106.
10. Veronesi U, Orecchia R, Luini A, et al. A preliminary report of intraoperative radiotherapy (IORT) in limited-stage breast cancers that are conservatively treated. *Eur J Cancer*. 2001;37:2178–2183.
11. Björk P, Knöös T, Nilsson P, Larsson K. Design and dosimetry characteristics of a soft-docking system for intraoperative radiation therapy. *Int J Radiat Oncol Biol Phys*. 2000;47:527–533.
12. Beddar AS, Domanovic MA, Kubu M Lou, Ellis RJ, Sibata CH, Kinsella TJ. Mobile linear accelerators for intraoperative radiation therapy. *Assoc Perioper Regist Nurses J* 2001;74:700–705.
13. Palta JR, Suntharalingam N. A non-docking intraoperative electron beam applicator system. *Int J Radiat Oncol Biol Phys*. 1989;17:411–417.
14. Jones D, Taylor E, Travaglini J, Vermeulen S. A non-contacting intraoperative electron cone apparatus. *Int J Radiat Oncol Biol Phys*. 1989;16:1643–1647.

15. Carlson M, Hessler J, Grzetic S, Gupta N. Dosimetric evaluation of soft docking sensitivity on an INTRAOP Mobetron IORT device. *Med Phys*. 2015;42:3407.
16. NaturalPoint, Inc. Optical Tracking Solutions, Corvallis, OR, USA. http://naturalpoint.com/. Accessed March 1, 2017.
17. Hartenberg RS, Denavit J. *Kinematic Synthesis of Linkages*. San Francisco, CA: McGraw-Hill; 1964.
18. Kraft D. On converting optimal control problems into nonlinear programming problems. In: *Computational Mathematical Programming*. Berlin, Heidelberg: Springer Berlin Heidelberg; 1985: 261–280.
19. Uneri A, Schafer S, Mirota DJ, et al. TREK: an integrated system architecture for intraoperative cone-beam CT-guided surgery. *Int J Comput Assist Radiol Surg*. 2012;7:159.
20. Pieper S, Halle M, Kikinis R. 3D Slicer. *IEEE Int Symp Biomed Imaging Nano to Macro*. 2004;2:632–635.
21. Marinetto E. BiiGOptitrack Library. http://github.com/HGGM-LIM/BiiGOptitrack. 2015.
22. García-Vázquez V, Marinetto E, Santos-Miranda JA, Calvo FA, Desco M, Pascau J. Feasibility of integrating a multi-camera optical tracking system in intra-operative electron radiation therapy scenarios. *Phys Med Biol*. 2013;58:8769–8782.
23. Marinetto E, García-Vázquez V, Santos-Miranda JA, et al. Optical tracking system integration into IORT treatment planning system. In: Roa L, ed. *Mediterranean Conference on Medical and Biological Engineering and Computing*. Vol 25-28 sept. 25/09/2013. Sevilla, España: Springer; 2014:37–40. http://www.springer.com/gp/book/9783319008455. Accessed February 20, 2017.
24. Calvo FA, Marinetto E, García-Vázquez V, et al. Stereotactic image-guided intraoperative electron irradiation: proof of concept and clinical feasibility. *Radiother Oncol*. 2014;1802:S117.
25. López-Tarjuelo J, Bouché-Babiloni A, Santos-Serra A, et al. Failure mode and effect analysis oriented to risk-reduction interventions in intraoperative electron radiation therapy: the specific impact of patient transportation, automation, and treatment planning availability. *Radiother Oncol*. 2014;113:283–289.